

Model-based ROC (mROC) curve: examining the effect of case-mix and model calibration on the ROC plot

Mohsen Sadatsafavi^{1,2}, Paramita Saha-Chaudhuri³, John Petkau⁴

1. Faculty of Pharmaceutical Sciences, The University of British Columbia
2. Faculty of Medicine, The University of British Columbia
3. Department of Epidemiology, Biostatistics and Occupational Health, McGill University
4. Department of Statistics, The University of British Columbia

Corresponding Author:

Mohsen Sadatsafavi
Associate Professor, Faculty of Pharmaceutical Sciences
The University of British Columbia
<http://resp.core.ubc.ca/team/msafavi>
msafavi@mail.ubc.ca

Word count: 5,223

Abstract word count: 292

Keywords: Clinical prediction models; Receiver Operating Characteristic; Model Calibration; Model Validation

Abstract

The performance of a risk prediction model is often characterized in terms of discrimination and calibration. The Receiver Operating Characteristic (ROC) curve is widely used for evaluating model discrimination. When comparing the ROC curves between the development and an independent (external) validation sample, the effect of case-mix makes the interpretation of discrepancies difficult. Further, compared to discrimination, evaluating calibration has not received the same level of attention in the medical literature. The most commonly used graphical method for model calibration, the calibration plot, involves smoothing or grouping of the data, requiring arbitrary specification of smoothing parameters or the number of groups.

In this work, we introduce the 'model-based' ROC (mROC) curve, the ROC curve that should be observed if the prediction model is calibrated in the external population. We first show that moderate calibration (having a response probability of $p\%$ among patients with a predicted risk of $p\%$) is a sufficient condition for convergence of the empirical ROC and mROC curves. We further show that equivalence of the expected values of the predicted and observed risk (mean calibration, or calibration-in-the-large) and equivalence of the mROC and ROC curves together guarantee moderate calibration. We demonstrate how mROC separates the effect of case-mix and model mis-calibration when comparing ROC curves from different samples. We also propose a test statistic for moderate calibration, which does not require any arbitrary parameterization. We conduct simulations to assess small-sample properties of the proposed test. A case study puts these developments in a practical context. We conclude that mROC can easily be constructed and used to interpret the effect of case-mix on the ROC curve and to evaluate model calibration on the ROC plot.

Background

Risk prediction models that objectively quantify the probability or rate of clinically important events based on observable characteristics are critical tools for efficient patient care. A risk prediction model is typically constructed in a development sample, but before it is adopted for use, its performance needs to be assessed in an independent (external) validation sample. In examining validity, two fundamental aspects are discrimination and calibration. The former refers to the capacity of the model to properly stratify individuals with different risk profiles, and the latter refers to the degree to which predicted risks are close to their true counterparts(1).

The Receiver Operating Characteristic (ROC) curve and its associated area under the curve (AUC, also known as the c-statistic) are classical examples of tools for assessing model discrimination. The ROC curve is often examined during both model development and validation, but the ROC curve based on the development sample and the ROC curve based on the validation sample may exhibit significant discrepancy. One area of interest in the present work is to understand the sources of discrepancy between the development and validation ROC curves. Previous work in this area has largely focused on the c-statistic, an overall summary measure of the ROC curve(2–4). It has been argued that the discrepancy in c-statistic between the development and validation samples can have two major sources: potential differences in the distribution of predictor variables (case-mix), and potential misspecification of the risk prediction model in the validation sample(3). As the former is a property of the sample, while the latter is an integral component of model validity, discerning these two sources of discrepancy can be informative.

Further, a crucial step when externally validating a risk prediction model is the assessment of its calibration. Compared to model discrimination, examining model calibration has not received the same level of attention(5,6), and for this reason, is referred to as “the Achilles’ heel of predictive analytics”(7). In the context of a logistic regression model for binary responses, Van Calster et al proposed a hierarchy of definitions for model calibration, with the first being the equivalence of the average values of the predicted and observed risks (mean calibration, or

calibration-in-the-large)(8). Weak calibration is achieved when there is no systematic overestimation or underestimation of risks at any levels of the predicted risk. Beyond this, a model is moderately calibrated if the average observed risk among all subjects with a given predicted risk is equal to the predicted risk. Finally, strong calibration is the equality of predicted and observed risks for each and every covariate pattern. However, Van Calster et al argue that strong calibration is unrealistic in practical situations. They show that moderate calibration is enough for a risk prediction model not to be associated with harm, and argue that aiming for moderate calibration is the most pragmatic approach in risk prediction(8). Moderate calibration is typically assessed using the calibration plot, which visualizes the average value of the observed risk as a function of the predicted risk after grouping or smoothing the response values.

In this manuscript, we extend the previous work on model-based or case-mix-adjusted c-statistic to the entire ROC curve by proposing the model-based ROC (mROC) analysis. Instead of focusing on a summary measure, mROC enables investigators to disentangle the effect of case-mix and model validity on the shape of the entire ROC curve during external validation. Importantly, we show that moderate calibration is a sufficient condition for the convergence of empirical ROC and mROC curves in an independent sample. As such, the mROC connects the ROC analysis, a classical means of evaluating model discrimination, to model calibration. We use this connection to propose a novel test for statistical inference on model calibration based on mROC. The proposed test has two attractive properties: it can be performed alongside the popular and familiar ROC curve analysis, and it does not require specifying arbitrary quantities such as a smoothing bandwidth or the number of groups, as is required for traditional model calibration measures.

Notation and context

Our proposed methodology is applicable in a setting where the objective is to validate a previously developed risk prediction model for a binary outcome in a representative, independent ‘external’ sample. In the external dataset, let $\mathbf{Y} = (Y_1, \dots, Y_n)$ be the binary outcome (or response) values (e.g., whether the disease will flare up in the next six months) for

a random sample of n independent individuals, with $Y = 1$ indicating presence of disease and $Y = 0$ indicating absence of disease. Through a previously developed risk prediction model, we obtain $\boldsymbol{\pi}^* = (\pi_1^*, \dots, \pi_n^*)$, the vector of predicted risks from the model for this sample. In what follows, unless otherwise specified, by calibration we refer to moderate calibration, i.e., $P(Y = 1 | \pi^* = z) = z$.

The empirical ROC curve

Two fundamental probability distributions underlie the ROC curve for a risk prediction model: the distribution of the predicted risks among individuals who experience the event (positive individuals, or ‘cases’), and among individuals who do not experience the event (negative individuals, or ‘controls’). Let F_1 and F_0 represent the corresponding cumulative distribution functions (CDFs), and let Y be the binary event indicator:

$$F_1(t) = P(\pi^* \leq t | Y = 1),$$

$$F_0(t) = P(\pi^* \leq t | Y = 0).$$

Note that, the true positive (TP) and false positive (FP) probabilities are closely linked with the distribution of risk among the positive and negative individuals, respectively: $TP(t) \equiv P(\pi^* > t | Y = 1) = 1 - F_1(t)$, and $FP(t) \equiv P(\pi^* > t | Y = 0) = 1 - F_0(t)$. The population ROC curve induced by the risk prediction model $\boldsymbol{\pi}^*$ can be expressed as

$$ROC(t) = 1 - F_1(F_0^{-1}(1 - t)),$$

where $0 \leq t \leq 1$ is the false positive probability(9).

With the external dataset, consistent estimators for F_1 and F_0 can be obtained by averaging the indicators $I(\pi_i^* \leq t)$ for each of the positive and negative groups:

$$F_{1n}(t) = \frac{\sum_{i=1}^n \{I(\pi_i^* \leq t) \cdot Y_i\}}{\sum_{i=1}^n Y_i},$$

and

$$F_{0n}(t) = \frac{\sum_{i=1}^n \{I(\pi_i^* \leq t) \cdot (1 - Y_i)\}}{n - \sum_{i=1}^n Y_i},$$

to generate $ROC_n(t)$, the empirical ROC curve, as a consistent estimator of the population ROC curve(10,11).

The model-based ROC (mROC) curve

If the risk prediction model is calibrated, for the i^{th} subject in the external sample, $P(Y_i = 1|\pi_i^*) = \pi_i^*$; thus, the vector of observed response values is a random draw of independent Bernoulli trials from the vector of predicted risks. Given this, one can study the ‘expected’ ROC curve that can be constructed by generating such random responses. Let Y^* be a random realization of this potential outcome from the predicted risk of a randomly selected individual. The ROC-related CDFs for such potential outcomes are:

$$\bar{F}_1(t) = P(\pi^* \leq t | Y^* = 1),$$

and

$$\bar{F}_0(t) = P(\pi^* \leq t | Y^* = 0).$$

Application of Bayes’ rule leads to the following estimators in the external sample:

$$\bar{F}_{1n}(t) = \frac{\sum_{i=1}^n I(\pi_i^* \leq t) \cdot \pi_i^*}{\sum_{i=1}^n \pi_i^*},$$

and

$$\bar{F}_{0n}(t) = \frac{\sum_{i=1}^n I(\pi_i^* \leq t) \cdot (1 - \pi_i^*)}{n - \sum_{i=1}^n \pi_i^*}.$$

Hence, one can generate a ‘model-based’ ROC, $mROC_n(t)$, independently of the observed outcomes in the external sample, based on the CDFs \bar{F}_{1n} and \bar{F}_{0n} obtained by averaging the indicator functions $I(\pi_i^* \leq t)$ with weights of $\pi_i^* / \sum \pi_i^*$ and $(1 - \pi_i^*) / \sum (1 - \pi_i^*)$ for the i^{th} individual in the sample.

Note that, for evaluating the CDFs \bar{F}_{1n} and \bar{F}_{0n} , we use all subjects included in the validation sample; in contrast, only predicted risks from positive subjects are used to obtain F_{1n} whereas only predicted risks from negative subjects are used to obtain F_{0n} . The observed outcomes in the validation sample do not appear in the expression of \bar{F}_{1n} and \bar{F}_{0n} . Therefore, the behavior of these CDFs depends on the predicted risks and in turn on the case-mix of the validation sample, rather than the observed outcomes. This is in contrast with the empirical ROC, where observed outcomes and case-mix (via the predicted probability) are used explicitly to estimate \bar{F}_{1n} and \bar{F}_{0n} . This distinction motivates our proposal for using mROC to discern the impact of calibration as we describe below.

mROC and model calibration

The limiting forms of the estimated CDFs \bar{F}_{1n} and \bar{F}_{0n} for the mROC are identified in **Appendix 1**. An important consequence is that, provided that the risk model is calibrated, $ROC_n(t)$ and $mROC_n(t)$ converge to the same value at each point t , as n , the sample size in the external sample, approaches infinity. That is, moderate calibration is a sufficient condition for asymptotic convergence of the empirical ROC and mROC curves. On the other hand, while any transformation that preserves the ranking of predicted risks will result in the same ROC curve, the mROC curve is affected by the value of the risks and will generally change under such transformations. Thus, mis-calibrated models will generally result in divergent mROC and ROC curves.

To illustrate this, consider the simple situation when the true risk, represented by p , has a standard uniform distribution in the population:

$$\begin{aligned} p &\sim \text{uniform}(0,1), \\ Y &\sim \text{Bernoulli}(p). \end{aligned}$$

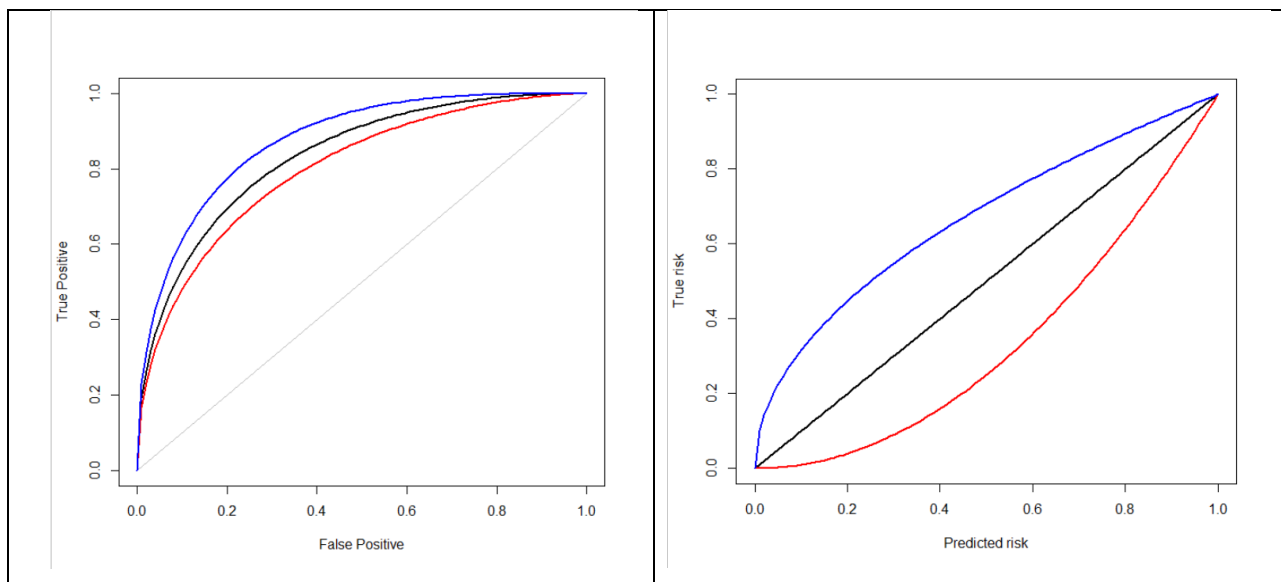
We consider three scenarios: the ‘correct specification’ scenario, when the prediction model correctly estimates the true risk ($\pi^* = p$) and thus is calibrated, and under two alternative scenarios of overestimation ($\pi^* = \sqrt{p}$) and underestimation ($\pi^* = p^2$) of the true risks. For

these three scenarios, the analytical forms of the population-based CDFs $F_1(t)$, $F_0(t)$, $\bar{F}_1(t)$, and $\bar{F}_0(t)$ are provided in **Table 1**.

Table 1: Population-based forms of the cumulative distribution functions underlying the empirical and model-based ROC curves for the simple uniform risk situation			
CDF	Scenarios		
	Correct specification	Overestimated risk	Underestimated risk
	$\pi^* = p$	$\pi^* = \sqrt{p}$	$\pi^* = p^2$
$F_1(t)$	t^2	t^4	t
$F_0(t)$	$2t - t^2$	$2t^2 - t^4$	$2\sqrt{t} - t$
$\bar{F}_1(t)$	t^2	t^3	$t^{3/2}$
$\bar{F}_0(t)$	$2t - t^2$	$3t^2 - 2t^3$	$(3\sqrt{t} - t^{3/2}) / 2$

For all three scenarios, given that the predicted risks are monotonically transformed versions of the true risk, the population-based ROCs are the same: $ROC(t) = 2\sqrt{t} - t$. However, $mROC(t) = ROC(t)$ only for the correct specification scenario. For the two alternative scenarios, closed-form expressions for $mROC(t)$ are not available, but the single root for $\bar{F}_0^{-1}(1 - t)$ can be found numerically to evaluate $mROC(t)$. Results are provided in **Figure 1**, where the ROC, mROC, and corresponding population-based calibration plots are provided for comparison. The latter have closed-form expressions in this simple situation, but in general calibration plots cannot be drawn without grouping or smoothing the data. On the other hand, the mROC curve can be evaluated from a sample without the requirement for any such arbitrary specifications.

Figure 1: ROC and mROCs for the simple uniform risk situation (left) and the corresponding calibration plots (right). Black: fully calibrated model; red: over-estimated risk; blue: underestimated risk. For the left panel, the ROC curves coincide (black line) for the three scenarios considered, but the mROC curves are distinct. For the right panel, the calibration curves for the three scenarios are all distinct.

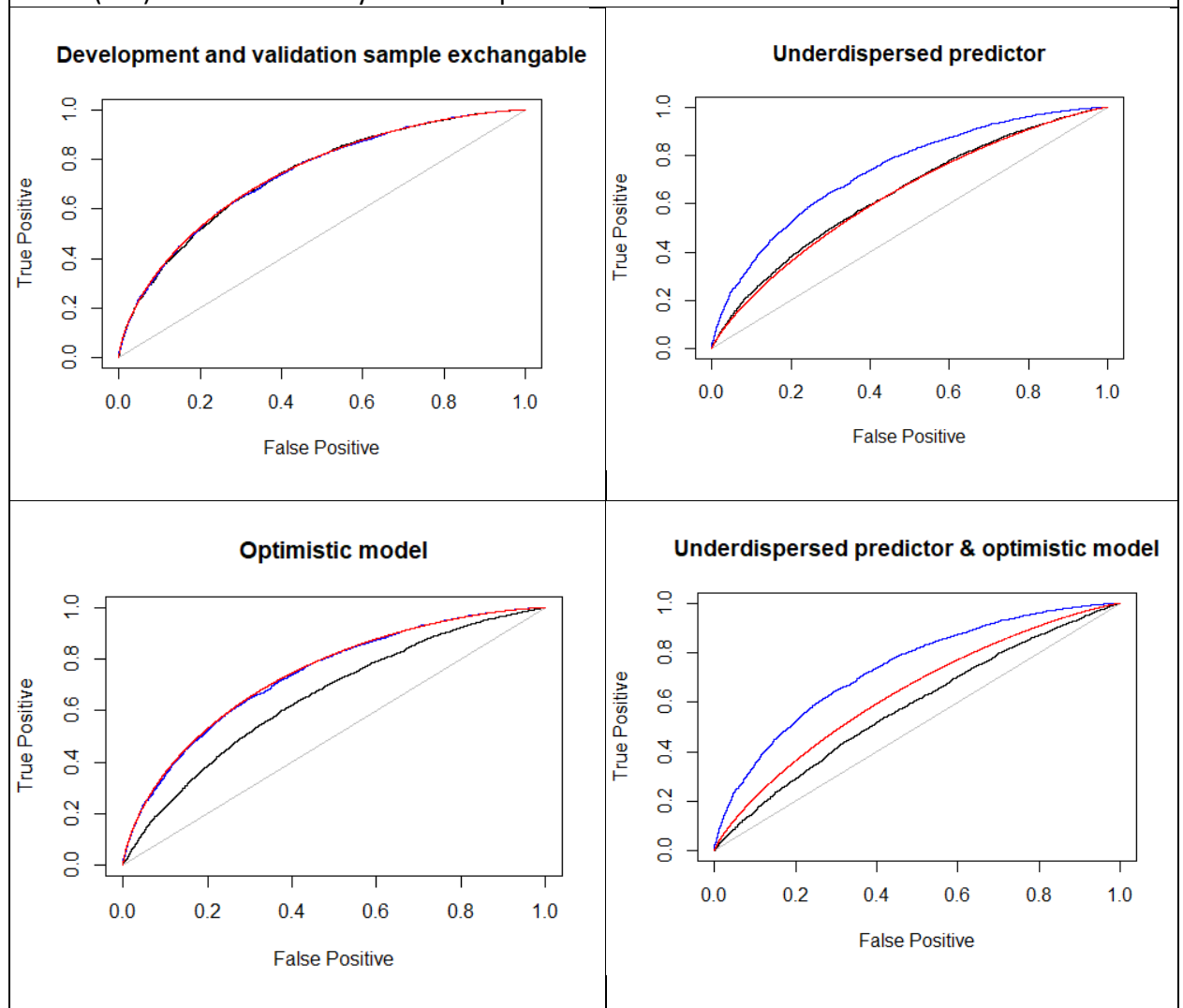


A graphical approach for separating the effect of case-mix and model calibration on the shape of ROC curve

Generally, two sources contribute to the shape of the ROC curve in the validation sample: the prediction model itself and the case-mix in the validation sample. Hence, the discrepancy between the development and external ROC curves can be affected by both the difference in case-mix and the calibration of the model in the samples. The following stylized example illustrates this. Consider a model with a single normally distributed predictor $X \sim \text{Normal}(0,1)$. Imagine using a development sample, we have constructed the risk model $P(Y = 1) = 1/(1 + \exp(-X))$, which happens to be the correct model (and thus is calibrated) in the development population. This model has a true c-statistic of 0.740. Now consider four hypothetical external validation scenarios. In the first (**Figure 2**, top-left), the development and validation samples are exchangeable. As such, the development and external ROC curves as well as the mROC curve all agree with each other. In the second scenario (**Figure 2**, top-right), the predictor is under-dispersed ($X \sim \text{Normal}(0,0.5)$) in the validation sample, while the model is still correct (and therefore is calibrated). Given the lower variance of the predictor, the true risks will have smaller variation in the validation sample. As expected, compared with the development ROC curve, the external ROC curve is closer to the diagonal line, with a c-statistic of 0.64. The mROC curve closely matches the external ROC curve, suggesting that the

discrepancy between development and external ROC curves is due to case-mix. Next, consider a validation population that has the same distribution of the predictor as the development population, but with a weaker predictor-outcome association: $P(Y = 1) = 1/(1 + \exp(-X/2))$. This represents a typical optimistic bias (the corresponding calibration plot would have a slope < 1). The weaker predictor-outcome association causes the external ROC curve to be closer to the diagonal line (**Figure 2**, bottom-left), with a c-statistic of 0.64. Here, the mROC curve remains close to the development ROC curve, indicating that the case-mix is similar between the two samples and the discrepancy between the development and external ROC curves is due to model mis-calibration in the validation sample. Finally, consider a scenario in which the predictor is under-dispersed ($X \sim \text{Normal}(0, 0.5)$) and the model is mis-calibrated (the association in the validation population is $P(Y = 1) = 1/(1 + \exp(-X/2))$) – **Figure 2**, bottom-right). Both factors contribute to the external ROC curve being closer to the diagonal line, with a c-statistic of 0.58. Here, due to the difference in the case-mix, the mROC departs from the development ROC curve, and due to the mis-calibrated model in the validation sample, it is not aligned with the external ROC curve either. This indicates that a mixture of case-mix difference and model mis-calibration is responsible for the discrepancy between the development and external ROC curves.

Figure 2: Empirical ROC in the development (blue) and external validation (black) datasets, and mROC (red) curves for the stylized example.



mROC as the basis of a novel statistical test for model calibration

As we demonstrate in **Appendix 1**, moderate calibration is a sufficient condition for the convergence at all points of the empirical ROC and mROC curves. However, moderate calibration on its own is not a necessary condition for such convergence. To progress, in **Appendix 2** we show that at the population level, the equivalence of ROC and mROC curves guarantees moderate calibration if an additional condition is imposed. This condition is mean calibration, i.e., $E(\pi^*) = E(Y)$, a condition whose assessment is an integral part of external validation of a risk prediction model(12).

While such equalities can hold at the population level, it is unrealistic to expect equivalence, either between the average predicted and observed risks, or between the empirical ROC and mROC curves, within a finite sample. Therefore, an objective assessment could be difficult to carry out in practice using the graphical approach described in the previous section. Instead, we propose a statistical inference procedure to test hypotheses about corresponding population quantities. We define the null hypothesis (H_0) as the model being calibrated: $P(Y = 1|\pi^* = z) = z$. Given the results in **Appendix 2**, H_0 can be seen as a combination of two null hypotheses, one on the equivalence of predicted and observed risks (H_{0A}), and the other on the equivalence of the mROC and ROC curves (H_{0B}):

$$H_0: \begin{cases} H_{0A} & E(\pi^*) = E(Y) \\ H_{0B} & \forall t \text{ mROC}(t) = \text{ROC}(t) \end{cases} \quad \begin{array}{l} \text{mean calibration} \\ \text{mROC and ROC equality.} \end{array}$$

Given the developments in **Appendix 2**, these hypotheses jointly provide the necessary and sufficient conditions for the risk prediction model to be calibrated.

For H_{0A} , consider $A = |E(Y) - E(\pi^*)|$. This population quantity achieves its minimum value of 0 if H_{0A} is true. Our proposed test statistic is the sample estimator of this quantity, the absolute average distance between the observed and predicted risks in the validation sample:

$$A_n = \frac{1}{n} \cdot |\sum_{i=1}^n (Y_i - \pi_i^*)| \quad (\text{mean calibration statistic}).$$

For H_{0B} , consider the population quantity $B = \int_0^1 |ROC(t) - mROC(t)|.dt$, which achieves its minimum value of 0 when the ROC and mROC curves are equal at all points. Our proposed test statistic is a sample estimator for this quantity, the integrated absolute difference between the empirical ROC and mROC curves in the validation sample:

$$B_n = \int_0^1 |ROC_n(t) - mROC_n(t)|.dt \quad (\text{ROC equality statistic}).$$

Given that both ROC_n and $mROC_n$ are step functions, the above integral is the sum of rectangular areas and can be precisely evaluated.

The distribution of B_n under the null hypothesis does not seem to be analytically tractable (for A_n , a Central Limit Theorem for independent but not identically distributed random variables indicates that with large enough samples, A_n will follow a half-normal distribution); but the null distributions of both A_n and B_n can be approximated numerically through straightforward Monte Carlo simulations. Through simulating vectors of response values from the vector of predicted probabilities, one can generate many simulated ROC curves and use them to construct empirical distribution functions under H_0 for A_n and B_n (the mROC curve is the same in all simulations as it is solely a function of predicted risks and not responses). These empirical distributions can then be used to generate approximate one-tailed p-values for these two statistics as:

$$p_{A_n} = 1 - eCDF_{A_n}(A_n),$$

where $eCDF_{A_n}$ is the empirical CDF of the mean calibration statistic under H_0 , and

$$p_{B_n} = 1 - eCDF_{B_n}(B_n),$$

where $eCDF_{B_n}$ is the empirical CDF of the ROC equality statistic under H_0 .

On their own, the two statistics provide insight about the performance of the model (one on mean calibration, and the other on the equivalence of mROC and ROC curves). Because testing mean calibration logically precedes the evaluation of moderate calibration, one can adopt a

sequential approach, testing H_{0A} of mean calibration first, and if H_{0A} is not rejected, proceeding to examine H_{0B} with the ROC equality test. The significance level of both tests can be modified to control overall type I error. However, it is more desirable to obtain a single overall p-value for H_0 .

If these tests were independent, one could use Fisher's method to obtain a unified p-value, based on the result that under H_0 , p_{A_n} and p_{B_n} have standard uniform distributions; thus the statistic

$$U_n = -2 \cdot [\log(p_{A_n}) + \log(p_{B_n})]$$

would have a chi-square distribution with 4 degrees of freedom(13). However, as the two statistics are generated from the same data, they are dependent. The adaptation of Fisher's method for dependent p-values can be used(14). This requires evaluating the expectation and variance of U_n under the null hypothesis, matching these moments to approximate the null distribution of U_n as that of a constant times a chi-square random variable, and modifying the test statistic and degrees of freedom of the chi-square reference distribution accordingly.

Because our Monte Carlo simulation provides many observations from the joint distribution of A_n and B_n , these correction factors can easily be obtained from the same simulated samples.

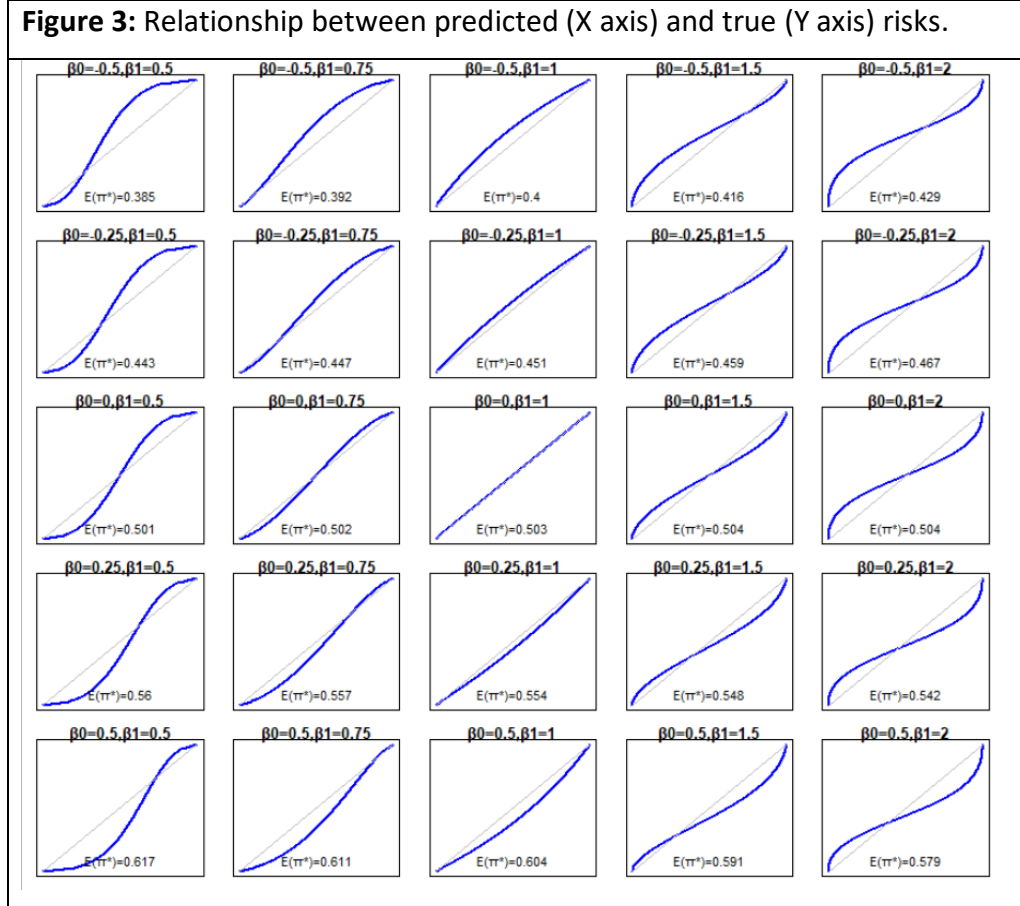
The steps for generating a unified p-value are outlined in the algorithm provided in

Supplementary Material – Section 1.

A brief simulation study

We have conducted simulation studies to evaluate the performance of our proposed test. The simulation setup was similar to the earlier stylized example: we modeled a single predictor X with a standard normal distribution, and the true risk as $p = 1/(1 + \exp(-X))$, resulting in the population average response probability of 0.5. We then evaluated the performance of the test in a simulated independent sample of n observations when the predicted risks suffer from various degrees of mis-calibration. This was modeled by applying a logit-linear transformation of the true risks to generate the predicted risks: $\text{logit}(\pi^*) = \beta_0 + \beta_1 \cdot \text{logit}(p)$. We simulated response values and predicted risks under a fully factorial design with values $\beta_0 =$

$\{-0.5, -0.25, 0, 0.25, 0.5\}$, $\beta_1 = \{0.5, 0.75, 1, 1.5, 2\}$, creating 25 simulation scenarios each for $n = \{100, 250, 1000\}$. **Figure 3** presents the population-level calibration plots for each of the 25 simulated scenarios.



We calculated the power of the mean calibration test, the ROC equality test, and the unified test in detecting mis-calibration, in terms of the proportion of times, out of 1,000 simulations, that the null hypothesis was rejected at the 0.05 significance level. Within each simulation, p-values were calculated with 100,000 Monte Carlo simulations. We used R for this analysis, with the implementation of the simulation-based estimation of $eCDF_{A_n}$ and $eCDF_{B_n}$ in C for computational efficiency.

Figure 4 provides the ROC and mROC curves. As all the mappings from p to π^* in these simulations are monotonic, the ROC curve remains the same in all panels (with a c-statistic of 0.74). However, the mROC is generally affected by the degree of mis-calibration. In particular,

higher values of β_1 result in a more concave mROC and a higher value of the area under the mROC curve. One exception is the third column, where $\beta_1 = 1$ (thus the predicted odds are proportional to the true odds). The mROC is not visibly affected by such a transformation.

Figure 4: ROC (black) and mROC (red) curves for the simulation scenarios. The panels positionally correspond to the calibration plots and simulation parameters presented in Figure 3.



The ROC curves approximate the population-level curves as they are based on a large sample size (10,000 simulated observations). The area under the ROC curve is 0.740 in all scenarios.

ROC: Receiver Operating Characteristic; B : ROC equality statistic; mAUC: area under the model-based ROC curve

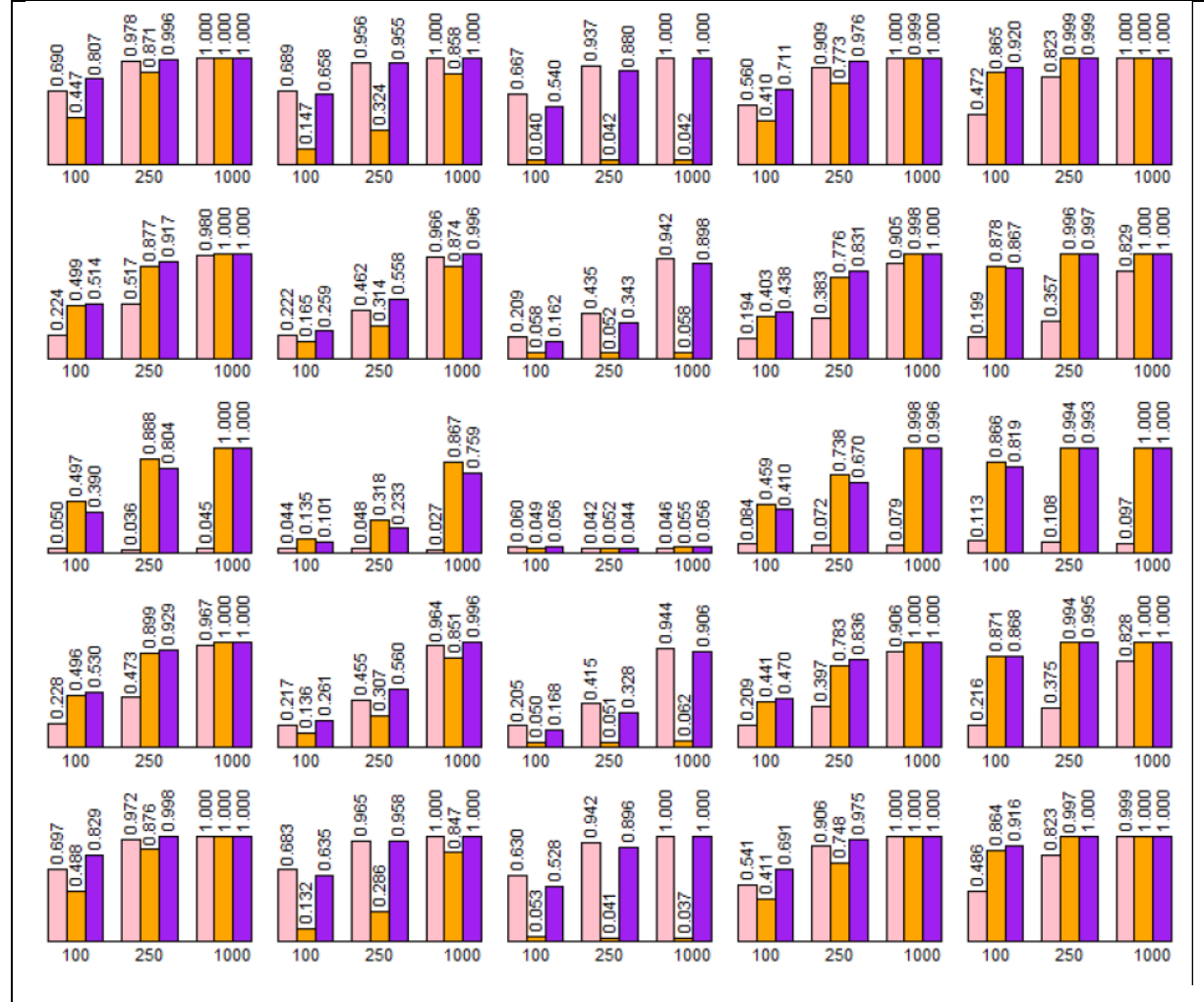
The performance of all three tests are summarized in **Figure 5**. The middle panel (third row and column), where $\beta_0 = 0$ and $\beta_1 = 1$, pertains to the only scenario where H_0 is true. All three

tests appropriately rejected the null hypothesis around their nominal significance level of 0.05.

The unified test was the only test that rejected H_0 with power >0.05 in all other scenarios.

Focusing on the third row, where $\beta_0 = 0$, given that the distributions of predicted risks are symmetric around 0.5, $E(\pi^*) = E(Y) = 0.5$ under these scenarios, and A_n fails. On the other hand, in the third column, where $\beta_1 = 1$ (thus the predicted odds are proportional to the true odds), B_n largely fails (the mROC and ROC curves are very close to each other under this scenario, as seen in **Figure 4**).

Figure 5: Probability of rejecting the null hypothesis for the mean calibration (pink bars), ROC equality (orange bars), and unified (purple bars) test statistics. The panels positionally correspond to the calibration plots and simulation parameters presented in Figure 3.



A second simulation was conducted by repeating these simulations with $X \sim \text{Normal}(-2,1)$, resulting in a population average response probability of 0.155. The results, provided in ***Supplementary Material – Section 2***, lead to similar conclusions.

Application

Chronic Obstructive Pulmonary Disease (COPD) is a common chronic disease of the airways characterized by progressive lung function decline and respiratory symptoms such as cough and shortness of breath. Periods of intensified disease activity, referred to as acute exacerbations, are an important feature of the disease and an important source of morbidity and mortality. Individuals vary widely in their tendency to exacerbate(15). Around 20% of exacerbations are severe, which means they require inpatient care(16). Predicting who is likely to experience an exacerbation, especially a severe one, will provide opportunities for preventive interventions. We demonstrate an application of mROC and our proposed test using data from two clinical trials of medications to prevent exacerbation in COPD patients.

MACRO was a clinical trial that investigated whether daily use of azithromycin, a broad-spectrum antibiotic, can decrease the rate of exacerbations(17). STATCOPE was a clinical trial of daily statin therapy for reduction of exacerbation rate(18). The benefit-harm of such preventive therapies can be more favorable in patients who will have more exacerbations in the future. As such, predicting the future exacerbation risk can enable more informed treatment decisions. We used data from MACRO to create a risk prediction model for the six-month risk of experiencing at least one exacerbation. We used the STATCOPE sample for external validation. Because dealing with the nuances of developing a risk prediction model is beyond the scope of this work, we have made simplifying assumptions and approaches (treating missing data and censoring as random, and not applying penalization in fitting the models). The resulting risk prediction model is for demonstration purposes only and must not be used for clinical decision making.

From the initial samples, 10 and 29 subjects in the development and validation samples, respectively, had missing predictors and were removed. Very few individuals (33 in the development and 16 in the validation samples) were censored during the first six months. For

simplicity, such individuals were removed from the study. The final samples included 1,074 subjects in the development and 832 subjects in the validation datasets. In the development dataset, 691 subjects (64.3%) had at least one exacerbation, and 141 (13.1%) experienced at least one severe exacerbation. In the validation sample, 454 subjects (54.5%) had at least one exacerbation, whereas 73 (8.8%) experienced at least one severe exacerbation.

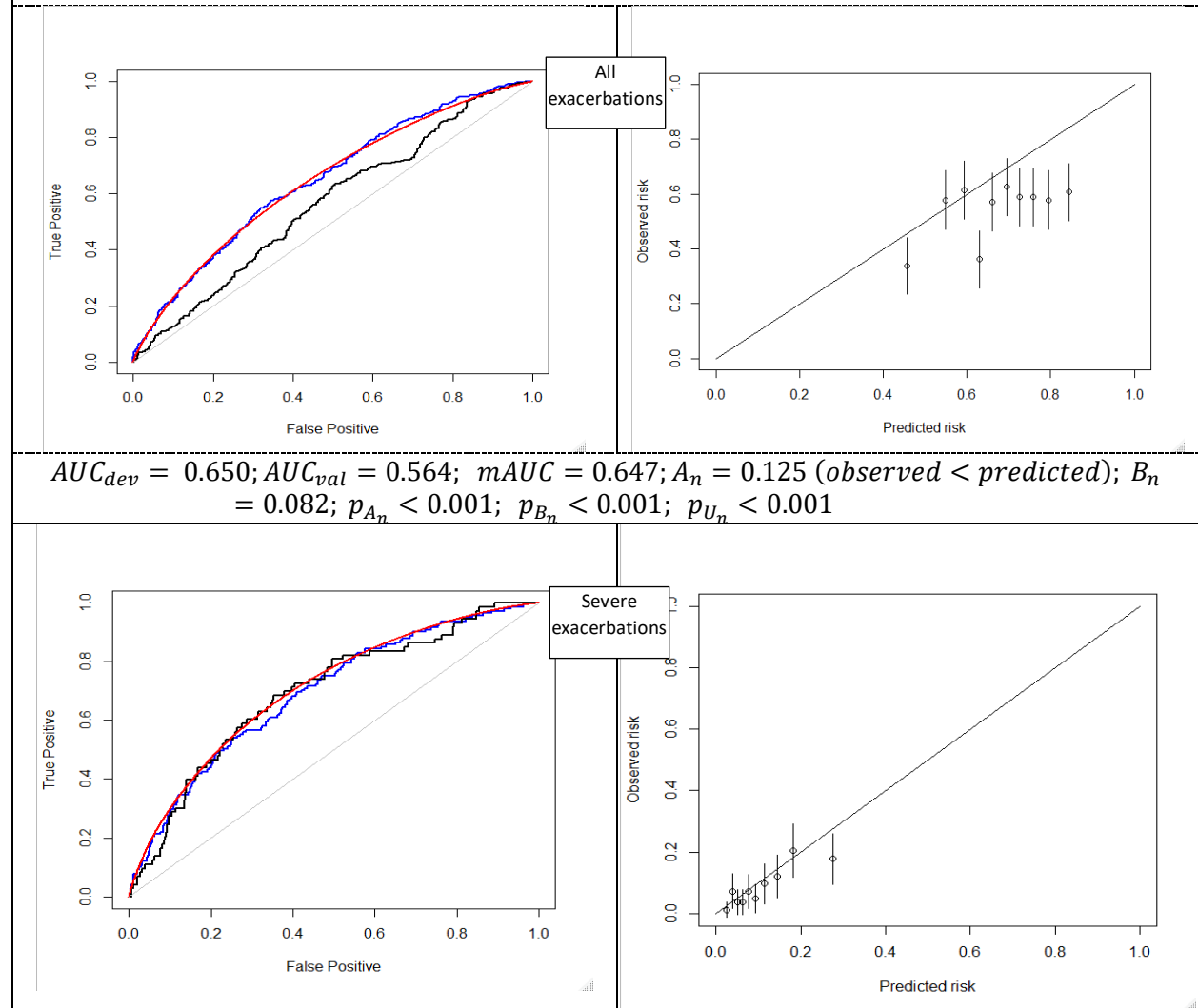
We used a logistic regression model that included the predictors as listed in **Table 2** based on a *priori* list of covariates selected based on prior knowledge of possible association with the outcome. We included a coefficient for randomized treatment (azithromycin) but it was set to 0 for prediction (as the model is applicable to those who are not on preventive therapy, and none of the individuals in the validation sample was on such a therapy). Maximum likelihood estimates of regression coefficients were used to construct the prediction score. We further developed a model only for severe exacerbations using the same approach. The linear predictors for both final risk prediction models are provided in **Table 2**.

Table 2: Regression coefficients of the risk prediction models for all and severe exacerbations within six months		
	All exacerbations Estimate (SE)	Severe exacerbations Estimate (SE)
Intercept	0.787 (0.707)	-3.840 (1.018)
Female sex	-0.482 (0.145)	0.209 (0.201)
Age (/10)	-0.094 (0.084)	-0.016 (0.119)
Previous history of oxygen therapy	0.275 (0.147)	0.297 (0.217)
Previous hospitalization	0.490 (0.135)	0.925 (0.200)
SGRQ	0.098 (0.043)	0.219 (0.063)
FEV ₁ (liters)	-0.158 (0.146)	-0.251 (0.219)
Current smoker	-0.168 (0.176)	-0.017 (0.242)
Current LABA user	0.157 (0.155)	0.466 (0.247)
Current LAMA user	0.354 (0.142)	0.083 (0.206)
SE: standard error; SGRQ: St. George Respiratory Questionnaire; FEV₁: Forced expiratory volume at one second; LABA: long-acting beta agonists; LAMA: Long-acting anti-muscarinic agents		

Figure 6 provides the empirical ROC curve from the development sample as well as the empirical ROC and mROC curves from the validation sample (left panels) and the calibration plot (right panels) for both outcomes. For overall exacerbations, the mROC curve was very close

to the development ROC curve but not to the external ROC curve. This indicates that the reduction in the discriminatory performance of the model is due to mis-calibration. Indeed, mean calibration was rejected ($\hat{E}(\pi^*) = 0.671$; $\hat{E}(Y) = 0.546$; $p_{A_n} < 0.001$; a two-tailed t-test also had $p < 0.001$), as well as the equivalence of the mROC and external ROC curves ($p < 0.001$). The unified test also rejected the hypothesis that the model is calibrated ($p < 0.001$). The calibration plot showed severe mis-calibration in the validation sample, with a general overestimation of the risk.

Figure 6: The empirical ROC curves from the development (blue) and validation (black) samples, the mROC curve from the validation sample (red) (left panel) and the calibration plot (right panel).



$AUC_{dev} = 0.692; AUC_{val} = 0.693; mAUC = 0.707; A_n = 0.019$ (<i>observed < predicted</i>); $B_n = 0.022; p_{A_n} = 0.071; p_{B_n} = 0.735; p_{U_n} = 0.202$
AUC_{dev} : area under the curve (c-statistic) in the development sample; AUC_{val} : area under the curve (c-statistic) in the validation sample; $mAUC$: area under the model-based ROC curve; A_n : Mean calibration statistic; B_n : ROC equality statistic; p_{A_n} : p-value of the mean calibration test; p_{B_n} : p-value for the ROC equality test; p_{U_n} : p-value of the unified test

The model for severe exacerbations had higher discriminatory power compared with all exacerbations. All three ROC curves were generally aligned with each other. Here, mean calibration was not rejected at 0.05 level ($\hat{E}(\pi^*) = 0.107; \hat{E}(Y) = 0.088; p_{A_n} = 0.071$; a two-tailed t-test generated a p-value of 0.061). The ROC equality test was also not significant ($p=0.735$). The unified test for model calibration did not reject the hypothesis that the model is calibrated ($p=0.202$). The calibration plot demonstrated generally good agreement between the predicted and observed risks for all but the highest decile (**Figure 6**).

Discussion

Our contribution in this work was the introduction of model-based ROC (mROC) analysis, the ROC curve that should be expected if the model is at least moderately calibrated in an external validation sample. We showed moderate calibration is a sufficient condition for the convergence of empirical ROC and mROC curves. We extended these results by proving that together, mean calibration and the equivalence of mROC and ROC curves in the population, are sufficient conditions for the model to be at least moderately calibrated. To test for such an equivalence within a sample, we suggested a simulation-based test. These results yield two connected applications. First, the mROC can be used to examine the potential role of case-mix versus model calibration when evaluating the discriminatory performance of a risk prediction model in a new sample. Second, the mROC provides a novel method for statistical inference on model calibration. To the best of our knowledge, this is the first time that the ROC plot, a classical means of communicating model discrimination, has been connected to model calibration. Given the vast popularity of ROC curves compared with calibration curves, this has

the potential to facilitate examining model calibration, which is often neglected when developing risk prediction models(7).

In the context of logistic regression, there are several approaches to examine how well the model fits the data. Allison reviewed several such tests and classified them into measures of predictive power (metrics similar to R^2) and goodness-of-fit tests (e.g., the Hosmer-Lemeshow test)(19). Our proposed test assesses model calibration, which makes it partially related to the latter. The test that is the most associated with calibration plots is the Hosmer-Lemeshow test, which is criticized due to its sensitivity to the grouping of the data, and lack of information about direction of mis-calibration(19). Our proposed test is free from arbitrary grouping of the data or the choice of smoothing factors. It provides information on mean calibration as well as mROC and ROC curve compatibility, which can be interpreted separately. Our brief simulations empirically assessed the postulated properties of this novel test in various sample size settings.

The proposed methodology for examining model calibration can also be compared against scalar metrics that are applied to the calibration plot. One such metric is Harrell's Emax statistic, defined as the maximum absolute difference between the calibration plot and the diagonal line(20). Recently, Austin and Steyerberg proposed the integrated calibration index (ICI), the average absolute distance of the calibration plot from the diagonal line when the response values are smoothed, with weights given by the probability distribution of predicted risks(21). Both Emax and ICI require smoothing of the calibration plot. On the other hand, while Emax and ICI have direct interpretations on the calibration plot, the mROC methodology does not provide a similarly interpretable scalar index. Rather, it breaks up the calibration assessment into the two metrics of mean calibration and ROC/mROC compatibility, which are interpretable on their own. These previous authors did not discuss statistical inference for Emax and ICI. One can conceive asymptotic or simulation-based methods for determining the distribution of Emax and ICI under the null hypothesis that the model is calibrated. The comparative performance of such tests and our proposed test needs to be studied in the future.

In the developments proposed in this work, we focused on applying the mROC methodology to an independent validation sample. It will be tempting to compare the mROC and ROC curves

within the development dataset. In many situations (e.g., logistic regression models), maximum likelihood estimation guarantees mean calibration in the sample. As such, comparing the ROC and mROC curves in this case might seem sufficient for demonstrating moderate calibration. A visual comparison of the mROC and ROC curves in the development sample can indeed provide subjective clues about the compatibility of the model with the data (e.g., the choice of the link function). Care should be taken, however, in statistical inference for such a comparison. Given that the predicted probabilities are estimated from the same data, the vector of responses is not a random draw from the vector of predicted probabilities (a fundamental notion justifying the construction of mROC). As such, the distribution of the p-values for the mean calibration and ROC equality statistics under the null hypothesis will not be uniform.

There are several ways the proposed methodology can be extended. We only focused on binary outcomes without censoring. The ROC curve has been extended to categorical data(22), as well as to time-dependent data(23); similar developments can also be pursued for the mROC methodology. We considered it to be beyond the scope of this paper to compare the performance of the unified test of model calibration with other statistical tests that are related to this context. This can be pursued in future studies. Development of inferential methods that would not require Monte Carlo simulations can also be of potential value. For example, as the ROC curve can be interpreted as a CDF(9), non-parametric statistics based on the distance between empirical distributions can conceivably be developed to test the equivalence of mROC and ROC curves. However, the calculation of the simulation-based p-value for the ROC equality test is very fast (due to the ease by which random binary responses can be generated from predicted risks). Thus, Monte Carlo error can be made smaller than the error generated from applying asymptotic methods to a finite sample. Another area of inquiry is on the form of the ROC equality test. We chose a test statistic based on the integrated absolute distance between the ROC and mROC curves, because such a statistic is on the same scale as the AUC and its nominal value can therefore be intuitively interpreted as the extent of ROC/mROC incompatibility. However, other metrics such as mean square difference might have better statistical properties. Another research area is examining to what extent the mROC curve is affected by various types of mis-calibration (i.e., the transformation function that maps

calibrated to predicted risks). This can help investigators make informed decisions on whether and how to recalibrate the risk prediction model in the new sample. In our simulation studies, the mROC did not vary much when the predicted odds were proportional to the true odds even though the finite-sample mROC is not generally invariant to such a transformation. This might stem from the design parameters of our brief simulation studies and needs to be evaluated for the more general case.

One of the promises of Precision Medicine is to empower patients for making informed decisions based on their specific risk of outcomes(24). Basing medical decisions on mis-calibrated predictions can be harmful. Our contribution is the development of mROC analysis, a simple method for separating the effect of case-mix and model mis-calibration on the ROC curve when externally validating a risk prediction model. We hope this development will further promote attention to model calibration by the applied health research community.

Acknowledgement

We would like to thank Dr. Abdollah Safari and Mr. Harry Lee, The University of British Columbia, for their insightful comments on earlier drafts.

Appendix 1

Lemma: For a moderately calibrated risk prediction model, the empirical and model-based ROC curves asymptotically converge.

Proof: A pre-specified risk prediction model $\pi^*(\mathbf{X})$ yields predicted risks $\pi_i^* \equiv \pi^*(\mathbf{X}_i)$, where \mathbf{X}_i is the vector of predictors for the i^{th} individual. When sampling from a population, the mapping from \mathbf{X}_i to π_i^* is known, but π_i^* for the i^{th} individual is random as \mathbf{X}_i is randomly selected. For any value of the predicted risk π^* , there is a unique ‘calibrated risk’ π given by the true risk of the outcome among all individuals with that predicted risk: $\pi \equiv \pi(\pi^*) = P(Y = 1 | \pi^*(\mathbf{X}) = \pi^*)$. A model is moderately calibrated when $\forall z, \pi(z) = z$.

We first consider the behavior of $F_{1n}(t)$. For each fixed value of t , $F_{1n}(t)$ is the average of $I(\pi_i^* \leq t)$ among individuals with $Y_i = 1$. Hence, provided $P(Y = 1) > 0$, dividing both the numerator and denominator of the expression for $F_{1n}(t)$ in the main text by n and applying the Weak Law of Large Numbers yields (in what follows, an arrow denotes convergence in probability as the sample size n approaches infinity), we have:

$$F_{1n}(t) \rightarrow \frac{E[I(\pi^* \leq t).Y]}{E(Y)} = \frac{P(\pi^* \leq t, Y = 1)}{P(Y = 1)} = P(\pi^* \leq t | Y = 1) = F_1(t).$$

Bayes' rule allows this limit to be re-expressed as:

$$P(\pi^* \leq t | Y = 1) = \frac{P(Y = 1 | \pi^* \leq t).P(\pi^* \leq t)}{P(Y = 1)}.$$

Proceeding similarly for $\bar{F}_{1n}(t)$ leads to:

$$\bar{F}_{1n}(t) \rightarrow \frac{E[I(\pi^* \leq t).\pi^*]}{E[\pi^*]} = \frac{P(\pi^* \leq t, Y^* = 1)}{P(Y^* = 1)} = P(\pi^* \leq t | Y^* = 1) = \bar{F}_1(t).$$

Again, applying the Bayes' rule, we have:

$$P(\pi^* \leq t | Y^* = 1) = \frac{P(Y^* = 1 | \pi^* \leq t).P(\pi^* \leq t)}{P(Y^* = 1)}.$$

For a moderately calibrated risk prediction model where $\pi(\pi^*) = \pi^*$, it follows immediately that $P(Y = 1) = E(\pi) = E(\pi^*) = P(Y^* = 1)$. To prove $F_{1n}(t) - \bar{F}_{1n}(t) \rightarrow 0$ we therefore only need to show that $P(Y = 1 \mid \pi^* \leq t) - P(Y^* = 1 \mid \pi^* \leq t) = 0$. But we have

$$P(Y = 1 \mid \pi^* \leq t) - P(Y^* = 1 \mid \pi^* \leq t) \propto \int_0^t \{P(Y = 1 \mid \pi^* = z) - P(Y^* = 1 \mid \pi^* = z)\} dP(\pi^* \leq z) = 0,$$

by the definition of moderate calibration.

Similar arguments apply for $F_{0n}(t)$ and $\bar{F}_{0n}(t)$, thereby establishing the desired result.

Appendix 2

Lemma: If the expected value of the predicted and true risks are the same in the population, then pointwise equality of population ROC and mROC curves implies the model is at least moderately calibrated.

Proof: Let $\pi^* = \pi^*(\mathbf{X})$ represent the predicted risk, and $G^*(\cdot)$ its CDF. Let $\pi(\cdot)$ be the true calibration function, representing the mapping from π^* to the actual risk: $\pi(z) = P(Y = 1 | \pi^* = z)$. A model being at least moderately calibrated means $\pi(z) = z$ almost everywhere (a.e.) on the support of $G^*(\cdot)$.

Given that the result to be established is concerned with population quantities, in place of the CDFs $F_{1n}(t)$, $F_{0n}(t)$, $\bar{F}_{1n}(t)$, and $\bar{F}_{0n}(t)$ that underlie the empirical ROC and mROC curves, we use the limiting versions of these CDFs.

For the ROC curve, we can express the underlying CDFs as

$$F_1(t) = P(\pi^* \leq t | Y = 1) = \frac{P(\pi^* \leq t, Y = 1)}{P(Y = 1)} = \frac{E[I(\pi^* \leq t) \cdot \pi(\pi^*)]}{E[\pi(\pi^*)]} = \frac{\int_0^t \pi(u) \cdot dG^*(u)}{\int_0^1 \pi(u) \cdot dG^*(u)},$$

and similarly,

$$F_0(t) = \frac{\int_0^t (1 - \pi(u)) \cdot dG^*(u)}{1 - \int_0^1 \pi(u) \cdot dG^*(u)}.$$

For the mROC curve, similar derivations result in

$$\bar{F}_1(t) = \frac{\int_0^t u \cdot dG^*(u)}{\int_0^1 u \cdot dG^*(u)},$$

and

$$\bar{F}_0(t) = \frac{\int_0^t (1 - u) \cdot dG^*(u)}{1 - \int_0^1 u \cdot dG^*(u)}.$$

For the sake of simplicity and avoiding technicalities around the behavior of the quantile function for discrete distributions, the proof presented here is for the common case where $G^*(\cdot)$ is a strictly increasing function without jumps (equivalently, it has a corresponding probability

density function having no intervals with zero density). This is the case, for example, for typical logistic regression models when there is at least one continuous predictor with unrestricted range. Given this condition, $\bar{F}_1(t)$ and $\bar{F}_0(t)$ are strictly increasing (without jumps) on $[0,1]$ and, with the additional technical condition that $0 < \pi(z) < 1$ (the true risk is not strictly 0 or 1 at any level of predicted risk), so too are $F_1(t)$ and $F_0(t)$.

With these expressions, we can re-express the result to be established as

$$\begin{cases} \text{Condition 1: } \int_0^1 u. dG^*(u) = \int_0^1 \pi(u). dG^*(u) \\ \text{Condition 2: } \forall t \bar{F}_1(\bar{F}_0^{-1}(1-t)) = F_1(F_0^{-1}(1-t)) \end{cases} \Rightarrow \pi(z) = z \text{ a. e.}$$

Let $a = a(t) = \bar{F}_0^{-1}(1-t)$ and $b(t) = F_0^{-1}(1-t)$; it follows that $\bar{F}_0(a) = F_0(b)$. Then *Condition 2*, and the strictly increasing nature of the CDFs, imply:

$$\bar{F}_0(a) = F_0(b) \Leftrightarrow \bar{F}_1(a) = F_1(b).$$

The expressions above for these CDFs yield the equivalent statement (after making use of *Condition 1*) that:

$$\int_0^a (1-u). dG^*(u) = \int_0^b [1-\pi(u)]. dG^*(u) \Leftrightarrow \int_0^a u. dG^*(u) = \int_0^b \pi(u). dG^*(u),$$

or equivalently:

$$\int_0^a u. dG^*(u) = \int_0^b \pi(u). dG^*(u) \Leftrightarrow G^*(a) = G^*(b).$$

Let $G^{*-1}(\cdot)$ be the quantile function of $G^*(\cdot)$. Let x be a value in $[0,1]$, and let $a = b = G^{*-1}(x)$. Then because the right hand side of the above statement holds for any value of x , we can conclude

$$\forall x \int_0^{G^{*-1}(x)} u. dG^*(u) = \int_0^{G^{*-1}(x)} \pi(u). dG^*(u).$$

With a change of variable $y = G^*(u)$, this becomes:

$$\forall x \int_0^x G^{*-1}(y). dy = \int_0^x \pi(G^{*-1}(y)). dy,$$

implying that $\pi(z) = z$ almost everywhere on the support of $G^*(\cdot)$, the probability distribution of the predicted risks.

References

1. Steyerberg EW, Vickers AJ, Cook NR, Gerds T, Gonen M, Obuchowski N, et al. Assessing the performance of prediction models: a framework for traditional and novel measures. *Epidemiol Camb Mass*. 2010 Jan;21(1):128–38.
2. van Klaveren D, Steyerberg EW, Vergouwe Y. Interpretation of concordance measures for clustered data. *Stat Med*. 2014 Feb 20;33(4):714–6.
3. van Klaveren D, Gönen M, Steyerberg EW, Vergouwe Y. A new concordance measure for risk prediction models in external validation settings. *Stat Med*. 2016 15;35(23):4136–52.
4. Gönen M, Heller G. Concordance probability and discriminatory power in proportional hazards regression. *Biometrika*. 2005 Dec 1;92(4):965–70.
5. Shah ND, Steyerberg EW, Kent DM. Big Data and Predictive Analytics: Recalibrating Expectations. *JAMA*. 2018 03;320(1):27–8.
6. Wessler BS, Paulus J, Lundquist CM, Ajlan M, Natto Z, Janes WA, et al. Tufts PACE Clinical Predictive Model Registry: update 1990 through 2015. *Diagn Progn Res*. 2017 Dec;1(1).
7. Van Calster B, McLernon DJ, van Smeden M, Wynants L, Steyerberg EW, Topic Group ‘Evaluating diagnostic tests and prediction models’ of the STRATOS initiative. Calibration: the Achilles heel of predictive analytics. *BMC Med*. 2019 Dec 16;17(1):230.
8. Van Calster B, Nieboer D, Vergouwe Y, De Cock B, Pencina MJ, Steyerberg EW. A calibration hierarchy for risk models was defined: from utopia to empirical data. *J Clin Epidemiol*. 2016;74:167–76.
9. Pepe MS, Cai T. The analysis of placement values for evaluating discriminatory measures. *Biometrics*. 2004 Jun;60(2):528–35.
10. Krzanowski WJ, Hand DJ. ROC curves for continuous data. Boca Raton: CRC Press; 2009. 241 p. (Monographs on statistics and applied probability).
11. Pepe MS. The statistical evaluation of medical tests for classification and prediction. 1. publ. in paperback. Oxford: Oxford Univ. Press; 2004. 302 p. (Oxford statistical science series).
12. Steyerberg EW, Vergouwe Y. Towards better clinical prediction models: seven steps for development and an ABCD for validation. *Eur Heart J*. 2014 Aug 1;35(29):1925–31.
13. Fisher RA. Statistical methods for research workers. 1930.
14. Brown MB. A Method for Combining Non-Independent, One-Sided Tests of Significance. *Biometrics*. 1975 Dec;31(4):987.

15. Sadatsafavi M, Sin DD, Zafari Z, Criner G, Connett JE, Lazarus S, et al. The Association Between Rate and Severity of Exacerbations in Chronic Obstructive Pulmonary Disease: An Application of a Joint Frailty-Logistic Model. *Am J Epidemiol*. 2016 Nov 1;184(9):681–9.
16. Aaron SD. Management and prevention of exacerbations of COPD. *BMJ*. 2014;349:g5237.
17. Albert RK, Connett J, Bailey WC, Casaburi R, Cooper JAD, Criner GJ, et al. Azithromycin for prevention of exacerbations of COPD. *N Engl J Med*. 2011 Aug 25;365(8):689–98.
18. Criner GJ, Connett JE, Aaron SD, Albert RK, Bailey WC, Casaburi R, et al. Simvastatin for the Prevention of Exacerbations in Moderate-to-Severe COPD. *N Engl J Med*. 2014 Jun 5;370(23):2201–10.
19. Allison PD. Measures of Fit for Logistic Regression [Internet]. Statistical Horizons LLC and the University of Pennsylvania; [cited 2020 Jan 13]. Report No.: 1485–2014. Available from: <https://support.sas.com/resources/papers/proceedings14/1485-2014.pdf>
20. Harrell FE. Regression modeling strategies: with applications to linear models, logistic and ordinal regression, and survival analysis. Second edition. Cham Heidelberg New York: Springer; 2015. 582 p. (Springer series in statistics).
21. Austin PC, Steyerberg EW. The Integrated Calibration Index (ICI) and related metrics for quantifying the calibration of logistic regression models. *Stat Med*. 2019 Sep 20;38(21):4051–65.
22. Li J, Fine JP. ROC analysis with multiple classes and multiple tests: methodology and its application in microarray studies. *Biostatistics*. 2008 Jul 1;9(3):566–76.
23. Saha-Chaudhuri P, Heagerty PJ. Non-parametric estimation of a time-dependent predictive accuracy curve. *Biostat Oxf Engl*. 2013 Jan;14(1):42–59.
24. Jameson JL, Longo DL. Precision Medicine — Personalized, Problematic, and Promising. *N Engl J Med*. 2015 Jun 4;372(23):2229–34.

Supplementary Material for

Model-based ROC (mROC) curve: examining the effect of case-mix and model calibration on the ROC plot

Mohsen Sadatsafavi; Paramita Saha-Chaudhuri; John Petkau

Table of content

Section 1: Calculating unified p-value for model calibration

Section 2: Results of the alternative simulation scenario

Section 1: Calculating a unified p-value for the assessment of model calibration

1. Calculate A_n and B_n from the vectors of $\boldsymbol{\pi}^*$ and \mathbf{Y} . These are the point estimates of the test statistics.
2. For $i=1$ to N (number of simulations):
 - 2.1. Generate a random response vector \mathbf{Y}_i^* from the predicted risks $\boldsymbol{\pi}^*$.
 - 2.2. Calculate A_{0i} and B_{0i} from $\boldsymbol{\pi}^*$ and \mathbf{Y}_i^* and store their values.
3. Based on the A_{0i} s and B_{0i} s, construct the empirical CDFs $eCDF_{A_n}(\cdot)$ and $eCDF_{B_n}(\cdot)$.
4. Calculate $p_{A_n} = 1 - eCDF_{A_n}(A_n)$, $p_{B_n} = 1 - eCDF_{B_n}(B_n)$, and $U_n = -2 \cdot [\log(p_{A_n}) + \log(p_{B_n})]$.
5. For each simulated vector \mathbf{Y}_i^* , use the same empirical CDFs to calculate simulated p-values p_{A_i} , p_{B_i} , and test statistic U_{n_i} . For these N values of U_{n_i} , calculate $c = \frac{var(U_n)}{2 \cdot average(U_n)}$ and $k = \frac{2 \cdot average(U_n)^2}{var(U_n)}$.
6. The unified p-value is evaluated as $p_{U_n} = 1 - F\left(\frac{U_n}{c}; k\right)$, where $F(\cdot; k)$ is the CDF of the chi-square distribution with k degrees of freedom.

Section 2: Results of the alternative simulation scenario

The simulation setup was similar to that of the main text. We modeled a single predictor $X \sim \text{Normal}(-2, 1)$, and the true risk as $p = 1/(1 + \exp(-X))$, resulting in the population average response probability of 0.155. We then evaluated the performance of the test in a simulated independent sample of n observations when the predicted risks suffer from various degrees of mis-calibration. This was modeled by applying a logit-linear transformation of the true risks to generate the predicted risks: $\text{logit}(\pi^*) = \beta_0 + \beta_1 \cdot \text{logit}(p)$. We simulated response values and predicted risks under a fully factorial design with values $\beta_0 = \{-0.5, -0.25, 0, 0.25, 0.5\}$, $\beta_1 = \{0.5, 0.75, 1, 1.5, 2\}$, creating 25 simulation scenarios each for $n = \{100, 250, 1000\}$. The ROC and mROC curves are presented in **Figure 2.1**. Results of the simulation studies, in terms of the proportion of times the null hypotheses were rejected, are provided in **Figure 2.2**.

Figure 2.1: ROC (black) and mROC (red) curves for the simulation scenarios. The panels positionally correspond to the calibration plots and simulation parameters presented in **Figure 3** in the main text.



Figure 2.2: Probability of rejecting the null hypothesis at 0.05 level for the mean calibration (pink bars), ROC equality (orange bars), and unified (purple bars) test statistics. The panels positionally correspond to the calibration plots and simulation parameters presented in Figure 2.1.

